

SPECTROPHOTOMETRY OF THE CRAB NEBULA AS A WHOLE

KRIS DAVIDSON

Astronomy Department, University of Minnesota, 116 Church Street, SE, Minneapolis, Minnesota 55455

Received 1 April 1987; revised 4 June 1987

ABSTRACT

A spatial scanning technique has been used to observe the visual-wavelength spectrum integrated over the Crab Nebula. The emission-line fluxes are useful for estimates of the nebular mass and chemical composition, while limits are placed on a possible emission-line halo around the Crab. One result is quite unexpected: Estimates of the [O III]/continuum flux ratio during the past 25 yr, including that presented here, are mutually discrepant, and one possible explanation is that the visual continuum of the Crab may be changing rapidly. This would have serious implications for models of the nonthermal SNR and pulsar. Particular types of observation are urgently needed in order to clarify the situation.

I. INTRODUCTION

The Crab Nebula is important partly because it is poorly understood. Unlike other young supernova remnants, it can be observed well enough at visual and ultraviolet wavelengths—the most critical wavelengths for analyzing “warm” SN debris—to reveal serious discrepancies between simple predictive theory and reality. Analyses of less observable SNRs therefore deserve skepticism until this object has been explained better. Modern ideas about the Crab have been reviewed by Davidson and Fesen (1985, hereafter referred to as DF) and by various authors in Kafatos and Henry (1985).

Some gaps in our knowledge are of course observational rather than theoretical. One instance is the lack of good spectrophotometry integrated over the entire Crab Nebula. As noted in DF, we need such observations for several applications: (1) A hypothetical circumnebular “halo” of thermal gas with either high or low velocity may be observable in the emission-line profiles. (2) The integrated hydrogen and helium emission-line fluxes are required for a nebular mass estimate. (3) The total emission-line spectrum is useful for assessing the overall chemical composition. (4) Secular changes in the continuum brightness may be detectable and would provide constraints on models of the nonthermal nebula. Reliable measurements for these purposes are difficult because the Crab has a fairly low surface brightness and is several arcminutes across, far too large to fit into the entrance apertures of modern instruments on large telescopes. Only a few relevant observations have been published. O'Dell (1962) used interference filters with photometers on small telescopes. Kirshner (1974) used a spectral scanner with a small objective lens, while Davidson, Crane, and Chincarini (1974) obtained digital images through interference filters on a large telescope. Clark *et al.* (1983) obtained high-resolution profiles of the [O III] emission lines at many locations which, in principle, can be summed to represent the whole nebula. The observations by O'Dell, by Kirshner, and by Davidson, Crane, and Chincarini had poor spectral resolution and inadequate signal/noise ratios, and Kirshner's absolute continuum measurements disagreed with O'Dell's by as much as 25%. The data of Clark *et al.* referred only to [O III] emission and apparently were not summed over the whole nebula. Thus we need better, more complete data.

Observations of a relevant type are reported in this paper. A telescope of moderate size was scanned back and forth across the Crab while collecting spectrophotometric data,

giving results that pertain to the entire nebula. This approach does not represent the best possible solution to the problem, but it uses readily available equipment and it works. Results on the emission-line spectrum and limits on a halo are major improvements over previous data and are mostly unsurprising. The observed continuum/emission-line ratios, however, are unexpectedly different from previous estimates in a way that is not easy to explain. It seems possible that a real change has occurred in the Crab.

The observations and data reduction are described in Sec. II below. Section III is a discussion of the nebular velocity distribution and limits on circumnebular halo gas, while Sec. IV is concerned with emission-line fluxes. The surprising continuum measurements are discussed in Sec. V. Finally, Section VI is a brief summary and discussion urging particular types of additional work.

II. THE OBSERVATIONS

The 1.5 m telescope and IDS at Mount Lemmon Observatory were used in January 1985 for this project. The IDS collected data simultaneously in two spectrograph apertures centered about 72" apart along an east–west direction. The dispersion direction was north–south. Each aperture was defined by superimposing an east–west slit, 6.7" wide, on a 13.5" circular aperture; this gave the maximum aperture area consistent with good spectral resolution. In terms of spatial coverage, each aperture was roughly equivalent to a 6.7" × 12.9" rectangle whose long axis was east–west. However, the slit width was uncertain by several percent. This geometrical arrangement was not optimal for the task (a slit with a two-dimensional detector would have been far more efficient) but was dictated by practical constraints.

Each data set referring to the whole Crab Nebula comprised a number of individual IDS integrations. During each integration, typically 4–8 min long, the telescope was systematically drifted in right ascension, making two to six passes along an east–west strip while collecting data separately in both apertures. (A drift direction parallel to the dispersion, i.e., north–south for these observations, would have been better in some ways but was not feasible with the Mount Lemmon telescope and IDS.) Strips covered in some data sets were widened by slightly changing the declination between passes in each integration, and in other cases the telescope was defocused for the same purpose. Including the effects of aperture size, seeing, adjustments in declination, and defocusing, individual strips observed in this way were 85" to 420" long (east–west) and 10" to 32" wide (north–

south). Because the telescope did not have satisfactory offset controls, the drift speed and position of each observation were calibrated by measurements of stars on a TV monitor and may be uncertain by about $\pm 3''$. However, because so many passes were made across the nebula, on several different nights, the overall coverage must have been quite representative. (The overall results are essentially averages over so many sample locations that uniformity in sample spacing is not very critical, except for the absolute flux calibration. The sample spacing was "blind" in the sense that there was no preference for either bright filaments or faint regions in the Crab, except that some data sets excluded the outer parts of the nebula as specified below.) Usually, during each night the first, fourth, seventh, etc., integrations pertaining to the Crab were done at various "sky" positions located between $250''$ and $350''$ from the center of the nebula.

The data were reduced in a conventional manner, including sky subtraction, correction for atmospheric extinction, and flux calibration by reference mainly to the stars Feige 15 and Feige 34 (Stone 1977). Efforts were made to reduce artificial waviness in the flux calibration as discussed by Davidson and Kinman (1985). The linearity of the IDS response was tested as described in Sec. V below.

The Crab data sets are listed in Table I. Data sets 1 and 2 were experimental and cover irregular, fairly random locations within the inner dashed outline in Fig. 1. Data sets 3 and 4 each include ten zones as shown in Fig. 2, almost covering the visible nebula and completely covering the bright parts of it. The large round shape outlined in Figs. 1 and 2 shows the boundary of faint [O III] emission in an image published by Gull and Fesen (1982); this extends farther out than the boundary in a deep continuum image by Scargle (1970). Data sets 5 and 6, intended to sample the generally brighter thermal emission in central parts of the nebula, include six sample regions shown in Fig. 1, with each spectrograph aperture covering half of each sample. The telescope was defocused so that star images were about $20''$ across, while data sets 5 and 6 were obtained. Locations where sky samples were taken are too numerous to show clearly in Figs. 1 and 2 (no two sky samples were taken at the same location), but were randomly located all around the Crab.

Data sets 1, 4, and 5 are second-order spectra with resolution between 5 and 6 Å (FWHM), intended to provide good [O III] line profiles. The other data sets are first-order spectra with resolution between 15 and 20 Å. In most cases, blocking filters were used to eliminate extraneous spectral orders, the only exception being data set 1, wherein strong first-order 8400–8800 Å night-sky emission degraded the 4200–4400 Å second-order data. The short-wavelength end of data set 3 is only marginally useful, because the Mount Lemmon IDS is quite insensitive at wavelengths shorter than 4000 Å.

TABLE I. Observations of the Crab Nebula at Mount Lemmon.

Data set	Date (UT) 1985	Wavelength coverage (Å)	Spatial coverage	Integration time (min)
1	Jan. 18	4200–5120	Irregular (Fig. 1)	105
2	Jan. 19	4340–7600	Irregular (Fig. 1)	135
3	Jan. 20	3570–6980	"Zones" (Fig. 2)	80
4	Jan. 21	4300–5220	"Zones" (Fig. 2)	80
5	Jan. 21	4300–5220	"Samples" (Fig. 1)	50
6	Jan. 22	4880–8150	"Samples" (Fig. 1)	50

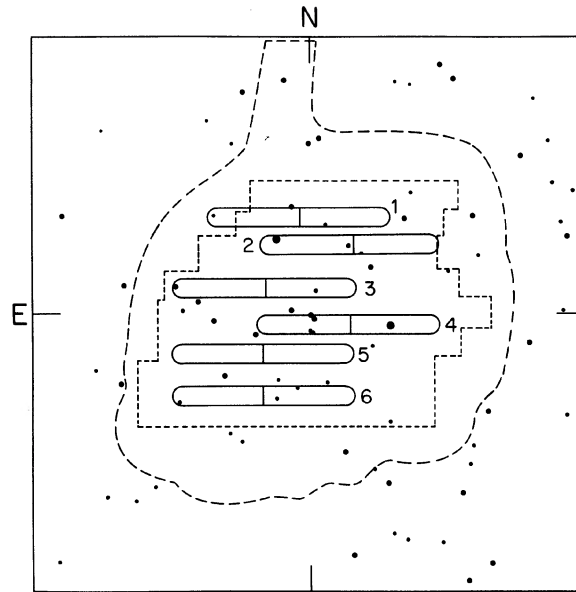


FIG. 1. Map indicating regions observed for data sets 1, 2, 5, and 6. The borders indicate a square $8'$ across, centered on the star $5''$ NE of the pulsar; dark circles represent stars. The large dashed, curved outline is the boundary of the nebula in [O III] emission according to Gull and Fesen (1982); the conspicuous bright nebular filaments do not extend so far out. Spatial coverage for data sets 1 and 2 was irregular and fairly random within the inner dashed outline, which approximates the bright parts of the nebula. The numbered oblong shapes are the "samples" included in data sets 5 and 6.

Sky subtraction was satisfactory for the individual integrations of data sets 1–5, even though the sky samples could not be obtained simultaneously with the Crab observations. On the night when data set 6 was obtained, however, thin clouds and irregular night-sky fluctuations caused traces of

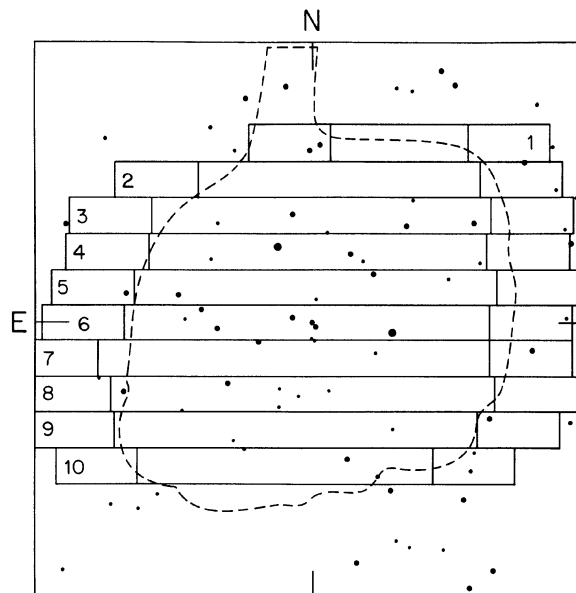


FIG. 2. Map indicating the "zones" observed for data sets 3 and 4. The rectangles at the ends of each zone were observed with only one spectrograph aperture each; the longer inner rectangles were observed with both spectrograph apertures. Each zone was covered in four east–west sweeps.

at least Hg λ 5460 and [O I] λ 5577, and possibly other features, to appear in the reduced data. (Because the relative brightnesses of such lines varied from sample to sample during that night, they could not be removed simply by renormalizing the night-sky data.) In data sets 3 and 4, the night-sky continuum was brighter than the Crab's continuum by a factor of about 2.

The integration times listed in Table I include both apertures in most cases. For example, in the case of data set 3 the actual time spent integrating on the Crab was 40 min, effectively giving 80 min because there were two apertures. Total integration times on night-sky samples near the Crab are not included in Table I but were slightly less than those on the nebula itself.

Somewhat surprisingly, subsets of the data do not reveal dramatic differences between parts of the Crab—north versus south in particular. Perhaps this is because the signal/noise ratios were inadequate for faint emission lines in the data subsets. Only the complete data sets and the overall spectrum of the Crab will be discussed in the following three sections.

III. THE [O III] LINE PROFILE AND LIMITS ON POSSIBLE HALO EMISSION

Tracings of most of the data, including night-sky spectra, are shown in Figs. 3 and 4. There is no sign of either high- or low-velocity emission that might come from a halo around the Crab (see DF and references therein). In particular, the [O III] emission around 5060 Å suspected by Clark *et al.* (1983) is not confirmed. Some appropriate bright emission lines to examine are [O III] $\lambda\lambda$ 4959, 5007, which tend to represent hotter, less dense material than H α and the [N II] and [S II] features do.

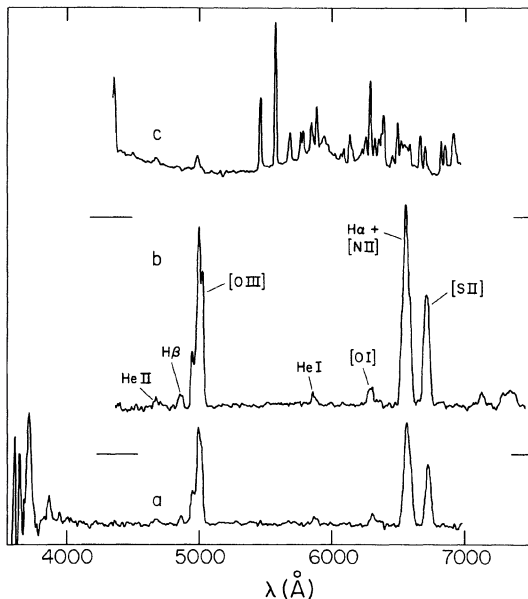


FIG. 3. (a) Tracing of the net sky-subtracted spectrum of the Crab in data set 3. (b) Tracing of data set 2. (c) Tracing of the average night-sky spectrum observed when data sets 2 and 3 were acquired. In each case F_{λ} , corrected for atmospheric extinction but not for interstellar extinction, is shown, although the units are not indicated. (For the night-sky spectrum, of course, the atmospheric extinction correction has no physical meaning.) Zero levels are indicated by horizontal lines.

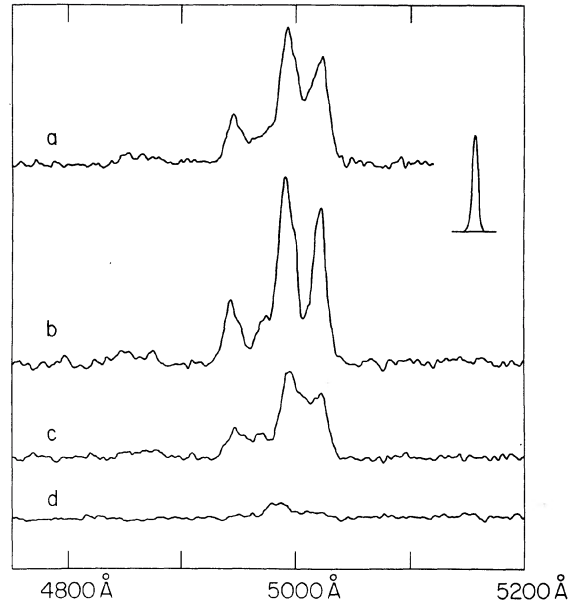


FIG. 4. Tracings of the [O III] region of the spectrum. (a) Data set 1. (b) Data set 5. (c) Data set 4. (d) Night-sky spectrum during the time when data sets 4 and 5 were acquired. The instrumental resolution profile is shown in the upper right-hand corner. Note that H β is very inconspicuous in these tracings. The bottom of the figure indicates the zero level for the night-sky spectrum; the other tracings are displaced vertically by arbitrary amounts.

Likely types of halo can be classified by expansion speed. Consider first the high-velocity case, with hypothetical ejection speeds of 4000–15000 km s⁻¹ in the supernova event. Such material would now be so extended that it would appear in the “sky” data taken about 300 arcsec from the center of the nebula, and would have been partly removed from the data on the Crab itself during the sky-subtraction process. Therefore we examine the background-sky data for features between 4750 and 5200 Å. A prominent feature between 4950 and 5030 Å (peak ~4980 Å, see Figs. 3(c) and 4(d)) is from high-pressure-sodium city lights; it appears also in data on other objects and fluctuated with a typical intensity of 2×10^{-16} erg cm⁻² s⁻¹ arcsec⁻² during the nights of observation. (Mount Lemmon is not a dark site.) Aside from this feature, the observed average night-sky spectrum associated with data sets 1 to 5, entailing several hours of integration time, is smooth enough to place a 2σ upper limit of roughly 4×10^{-17} erg cm⁻² s⁻¹ arcsec⁻² on high-velocity [O III] emission with radial-velocity dispersion ~4000 km s⁻¹, for example.

A moderate-velocity halo with speeds around 2500 or 3000 km s⁻¹ would not be extended enough to appear in the sky-background data. In this case we can examine wavelengths around 4915 and 5055 Å in data sets 1, 4, and 5 (Fig. 4). Almost no [O III] emission with speeds exceeding ± 1900 km s⁻¹ can be seen in the data. The integrated [O III] intensity between 5040 and 5065 Å, for instance, is less than 7×10^{-17} erg cm⁻² s⁻¹ arcsec⁻² at the 2σ level. Values quoted here have been corrected for atmospheric extinction but not for interstellar extinction.

As emphasized in DF, a low-velocity halo may exist if the presupernova star (perhaps a red supergiant?) ejected mate-

TABLE II. Relative line intensities (not corrected for interstellar reddening).

Emission line	Data set						(Kirshner 1974)
	1	2	3	4	5	6	
[O II] $\lambda\lambda$ 3726,3729	—	—	700?	—	—	—	500 \pm 60?
[Ne III] λ 3869	—	—	100?	—	—	—	—
He II λ 4686 (+ [Fe III]?)	55:	38:	40:	52:	—	—	—
H β λ 4861	50:	58:	48:	56:	62:	—	65 \pm 20
[O III] $\lambda\lambda$ 4959,5007	1000	1000	1000	1000	1000	1000	1000
He I λ 5876	—	40:	50:	—	—	53:	—
[O I] $\lambda\lambda$ 6300,6363	—	100	105	—	—	135:	—
H α λ 6563 + [N II] $\lambda\lambda$ 6548,6583	—	1120	1050	—	—	1100	1200 \pm 120
[S II] $\lambda\lambda$ 6716,6731	—	550	485	—	—	580	650 \pm 90
[Ar III] λ 7136	—	60:	—	—	—	70:	—
[O II] $\lambda\lambda$ 7319,7330 + [Ni II] λ 7378	—	160:	—	—	—	180:	—

rial for a long time before it exploded. Such a halo may be large enough to appear in the sky-background data and would be spectrally unresolved. Unfortunately, as mentioned above, a broad night-sky feature affects the relevant data at 5007 Å. The 2σ upper limit for a low-velocity λ 5007 “spike” is about 2×10^{-17} erg cm $^{-2}$ s $^{-1}$ arcsec $^{-2}$ in the sky data and higher by a factor of 2 or 3 in the sky-subtracted data sets 1, 4, and 5 (Fig. 4).

The [O III] halo intensity limits mentioned above are of the order of $10^{-15.8}$ erg cm $^{-2}$ s $^{-1}$ arcsec $^{-2}$ after correction for interstellar extinction (see Sec. IV below). The corresponding emission measure would be of the order of 5 pc cm $^{-6}$ for gas with solar H/He/O abundance ratios at a temperature of 15 000 K and with oxygen largely in the form of O $^{++}$. Such an emission measure is similar to values proposed, for example, by Chevalier (1977) and Murdin and Clark (1981) for a Crab halo. However, the assumptions made above are optimistic in the sense that they are favorable for [O III] emission. Oxygen may be ionized beyond O $^{++}$ in the rarefied gas around the Crab. Therefore He II λ 4686, as well as [O III] and H α emission, is worth investigating with long integration times. A more efficient way of detecting a *high-speed* halo would be to obtain images through interference filters, particularly in the wavelength range 5050–5150 Å for [O III].

The [O III] profiles in Fig. 4 contain information about the nebular velocity distribution. In each case the λ 4959 profile closely resembles that of λ 5007. The short-wavelength side of each line is brighter than the long-wavelength side (cf. Fig. 1(b) of Clark *et al.* 1983). Extinction by dust within the nebula is not a likely explanation for this asymmetry, because such extinction is very small except in the thickest nebular filaments (Woltjer and Véron-Cetty 1987; Trimble 1977). Since the negative radial velocities are smaller in size than the positive velocities, the *average* radial velocity relative to the Sun is not large despite the asymmetry of the [O III] profile. The average wavelength of the observed [O III] emission is 4994.4 Å with a rms deviation of only 0.5 Å among the data sets, where night-sky lines have been used to correct for flexure errors. If the zero-velocity average wavelength for [O III] $\lambda\lambda$ 4959,5007 is 4995.0 \pm 0.3 Å, and with a correction for the Earth’s motion, the average radial velocity of [O III] emission in the Crab is -55 ± 35 km s $^{-1}$ relative to the Sun. Although data set 5 appears to show a small amount of emission with radial velocities around -1800 and $+2100$ km s $^{-1}$, nearly all of the emission in each data set is between -1700 and $+1900$ km s $^{-1}$

relative to the Sun.

The deep central depressions in the [O III] profiles imply that there is little low-speed material in the Crab. The complete line profile of an expanding hollow shell would be flat-topped; but data sets 1 and 5, referring to the central part of the Crab’s projected image, exclude some material that is moving perpendicularly to the line of sight and therefore these data sets have little emission near zero radial velocity. (By the same reasoning, perhaps even data set 4 is not complete in its spatial coverage. However, this is not certain, since there is a perceptible intrinsic asymmetry in the Crab.) The radial velocities of the [O III] peaks in Fig. 4 are about -900 ± 25 km s $^{-1}$ and $+970$ km s $^{-1}$ (heliocentric). Evidently, there is a lack of material with expansion speeds less than 900 km s $^{-1}$, corresponding to a central cavity about 1.6 pc in diameter.

IV. EMISSION-LINE FLUXES

Table II shows relative line intensities measured in each data set. These values represent energy (not photon) fluxes, have been normalized to [O III] $\lambda\lambda$ 4959,5007 \equiv 1000, and have not been corrected for interstellar reddening. The [S II] values have been corrected slightly for He I λ 6678 emission, and in the λ 7350 feature the [O II] and [Ni II] contributions seem roughly equal, judging from that feature’s appearance. Relative line intensities estimated by Kirshner (1974) for the brightest lines are also listed in Table II.

Table III shows average values derived from Table II, as

TABLE III. Adopted relative line intensities for the entire Crab Nebula (Colons and question marks indicate increasing degrees of uncertainty.)

	Apparent	Corrected for $E_B - \nu = 0.47$
[O II] $\lambda\lambda$ 3726,3729	600	970?
[Ne III] λ 3869	100?	155?
He II λ 4686	40 \pm 8	45:
H β λ 4861	54 \pm 5	57
[O III] $\lambda\lambda$ 4959,5007	1000	1000
He I λ 5876	48 \pm 6	36:
[O I] $\lambda\lambda$ 6300,6363	110 \pm 15	75:
H α λ 6563	285 \pm 35	185:
[N II] $\lambda\lambda$ 6548,6583	800 \pm 40	510
[S II] $\lambda\lambda$ 6716,6731	530 \pm 40	330
[Ar III] λ 7136	65:	37:
[O II] $\lambda\lambda$ 7319,7330	90?	50?
[Ni II] λ 7378	80?	45?

suming informal but plausible relative weights for the data sets. Here the value for $H\alpha$ is indirectly guessed from the $H\beta$ intensity (see Miller 1978; Davidson 1979). In the last column of Table III, corrections have been made for interstellar reddening with $E_{B-V} = 0.47$ mag (see DF), using a reddening curve adapted from Savage and Mathis (1979) and Hayes *et al.* (1973). (*Caveat:* Comparisons with other [O II], [N II], and continuum estimates suggest that there may be a systematic “color” error in the flux calibration, of the order of 20% across the wavelength interval from 4000 to 7000 Å. For instance, the [O II]/[N II] ratio may be overestimated in Table III. If so, the effect in the last column of the table is the same as if E_{B-V} had been overestimated by about 0.1 mag. The possibility of a systematic color error in the flux calibration will be mentioned again at the end of Sec. V below.)

The overall nebular spectrum listed in Table III closely resembles a composite spectrum of a few particular filaments in the Crab, listed in Table 5 of Davidson (1979). A significant exception is He II λ 4686. Although this line is difficult to measure, the data suggest that the λ 4686/ $H\beta$ intensity ratio for the whole nebula is almost twice as large as it is for a typical bright filament. If true, this presumably indicates the presence of optically thin, highly ionized gas which is less dense than the more conspicuous filamentary cores (cf. remarks in Davidson *et al.* 1982, Pequignot and Dennefeld 1983, and Section 3 of DF). The large average [O III]/ $H\beta$ ratio is consistent with the same idea.

The helium/hydrogen line ratios in Table III indicate an average abundance ratio $n(\text{He}^+, \text{He}^{++})/n(\text{H}^+) \approx 0.57 \pm 0.08$ if we can neglect collisional excitation of He I λ 5876. With this assumption and also neglecting He⁰ (neither of which is really justified), one would guess the nebula to be about 70% helium by mass. See Section 3 of DF for a discussion of the complicating factors.

Data sets 3 and 4 almost cover the visible nebula and can be used to estimate total emission-line fluxes, even though the observing method used here is ill adapted to absolute flux calibration. Let us express the total apparent [O III] $\lambda\lambda$ 4959, 5007 flux, corrected for atmospheric extinction but not for interstellar extinction, in units of 10^{-10} erg cm^{-2} s^{-1} . Previous estimates of this flux were 1.9 units (O’Dell 1962) and either 2.1 or 2.0 units (Kirshner 1974, Tables 1 and 3, respectively), in each case with an expected uncertainty of $\pm 10\%$ or better. In the results reported here, assuming that each IDS spectrograph aperture area was 86 arcsec², the average [O III] intensity was 2.15×10^{-15} erg cm^{-2} s^{-1} arcsec⁻² in data set 3 and 10% less in data set 4. The total area covered by the zones in Fig. 2 is 1.06×10^5 arcsec². Multiplying this area by the average intensity in data sets 3 and 4, we find a total [O III] flux of about 2.15 units. This practically represents the whole nebula; the small northern and southern boundary regions that were not covered (Fig. 2) may be neglected because they include only 5% of the area within the Gull and Fesen (1982) [O III] boundary and are far below average in surface brightness or intensity. Various possible errors in the flux calibration are noted in Sec. V below; but evidently these have not caused much net error, because the deduced [O III] flux, 2.15 units, is reasonably consistent with O’Dell’s and Kirshner’s values, 1.9 to 2.1 units. This implied validity of the flux calibration is relevant to the continuum as discussed in Sec. V.

Emission-line luminosities are relevant to the question of nebular mass. Let us adopt 2.1×10^{-10} erg cm^{-2} s^{-1} for the

apparent [O III] flux from the Crab, consistent with the above discussion. Assuming a distance of 1830 pc and a correction factor of 4.6 for interstellar extinction (see DF), we find that the [O III] luminosity is about 3.9×10^{35} erg s^{-1} . Table III then implies that the $H\beta$ and He I λ 5876 luminosities are about 2.2×10^{34} and 1.6×10^{34} erg s^{-1} , respectively. The effect of these results on a nebular mass estimate is not straightforward and can only be alluded to here (see DF for an outline of the reasoning and likely mass values). Both $H\beta$ and He I λ 5876 appear to be somewhat fainter than previously supposed, and of course this tends to reduce the estimated nebular mass. However, the unusually large He II λ 4686/ $H\beta$ and [O III]/ $H\beta$ ratios imply the presence of much low-density material, which tends to increase the estimated mass. Additional observations and models of densities and ionization ratios are needed for a proper analysis.

V. THE NONTHERMAL CONTINUUM

A surprising result is found for the continuum brightness. Let us refer to the apparent continuum flux F_λ from the entire Crab Nebula at $\lambda = 5000$ Å, estimated using data in the wavelength range 4400–5600 Å. (F_λ is a more convenient quantity than F_ν or νF_ν for this purpose, because it is fairly “flat.” No corrections for interstellar extinction are applied in this section.) Our unit of measurement will be 10^{-12} erg cm^{-2} s^{-1} Å⁻¹. O’Dell (1962) found a value of 1.2 units, but Kirshner (1974) found a smaller flux, about 0.95 units, and the latter value was crudely confirmed to some extent by Davidson, Crane, and Chincarini (1974). Thus it seemed likely that O’Dell’s value had been an overestimate. However, the data reported here imply a smaller flux than even the 1974 value. With the same assumptions about flux calibration used for [O III] in Sec. IV above, one finds F_λ (5000 Å) ≈ 0.78 units in data set 3 and 0.68 units in data set 4. Assuming that data set 3 is better because its wavelength coverage is wider, we adopt the value 0.75 ± 0.07 units. Thus, three independent measurements at 12 yr intervals seem to have given a monotonic sequence 1.2, 0.95, 0.75 units, a decay rate of 2% per year. This is too rapid to be a long-term trend; at such a rate the Crab would have been a naked-eye object in the 18th Century! But temporary fluctuations at this rate may be possible, or alternatively, the “observed” decline may be real but slower than estimated here. A rate around 1% per year, for instance, would still be much faster than the rate of less than 0.2% per year observed at radio wavelengths (Aller and Reynolds 1985). It is interesting to note that the Crab *pulsar* has been fading in visual brightness at a rate between 0.5% and 1% per year (Kristian 1978; Middleditch *et al.* 1987).

Is the suspected trend in F_λ real? The previous measurements are difficult to assess. Likely errors in the continuum estimate reported here include the following:

(1) The flux calibration may be inadequate because the spectrograph aperture size and the spatial coverage of the nebula are imprecisely known. However, as reported in Sec. IV above, the [O III] emission flux estimated in the same way practically agrees with O’Dell’s and Kirshner’s results. To some extent, we can avoid absolute calibration by citing the [O III] equivalent width: 150 Å (O’Dell 1962), 210 Å (Kirshner 1974), 220 Å (Davidson, Crane, and Chincarini 1974), and 290 Å (data reported here). Of course, we do not know how steady the [O III] flux is; this depends on the gas distribution and on the ultraviolet ionizing flux. *But in any case the numbers seem to imply a large change in the [O III]/*

continuum brightness ratio, independent of flux calibration.

(2) The spatial coverage in data sets 3 and 4 is smaller than O'Dell's and Kirshner's. However, the visible emission-line nebula, which has fairly definite boundaries, is nearly covered (Fig. 2). If limited spatial coverage is the reason for the smaller continuum flux found here, then the [O III]/continuum brightness ratios may indicate that a *nonthermal continuum* halo, outside the visible [O III] nebula, was included in the earlier observations and not in those reported here. Images published by Scargle (1970) and by Gull and Fesen (1982) suggest the contrary, that [O III] emission is more extended than the visual-wavelength continuum nebula. A faint nonthermal halo may exist (cf. radio observations: Wilson and Weiler 1982; Matveenko 1984; Velusamy 1984), but is not expected to account for nearly 20% of the total visual-wavelength flux.

(3) Because the telescope pointing was imperfect, presumably there were nonuniformities in the sampling of the zones shown in Fig. 2. Some narrow east-west strips may have been missed while others would then have been sampled twice. However, such negative and positive errors probably cancelled each other quite well. Each east-west scan was roughly 8" wide in declination (spectrograph aperture width blurred by seeing) and there were four scans per zone so their interval (spacing between midlines) was also about 8". Note that exact equality between scan width and scan interval was not necessary, nor was it necessary for each scan to be exactly uniform in its spatial sensitivity distribution; the measurement procedure essentially involved sampling *average* intensities within a known area that included many scans. North-south position errors may have been 3" to 5" in some cases but not worse. Major spatial irregularities in the Crab are larger than the observational scale sizes quoted above, and there are enough irregularities and enough scans for statistical averaging. Therefore—although this cannot strictly be proven except by further observations—errors arising from nonuniform sampling should not have been worse than a few percent in the total flux estimates. This is particularly true of the [O III]/continuum ratio.

(4) Since the Crab's continuum is notoriously polarized, instrumental polarization must be considered for the data reported here and also for Kirshner's data, both of which employed grating spectrographs. However, the net continuum polarization of the entire nebula is only of the order of 9%, at position angle 160° (Oort and Walraven 1956). The dispersion direction in the Mount Lemmon data was near position angle 180°. For data set 3, instrumental polarization was probably less than 10% at $\lambda = 5000 \text{ \AA}$, near the grating blaze wavelength; the overall correction is therefore probably not worse than 1%. For data set 4, the grating polarization was around 20% at 5000 \AA , leading to a 2% overestimate of the Crab's brightness. This is negligible compared to other likely errors.

(5) In principle, the sky-subtraction process used here was dangerous because sky sampling was not simultaneous with observations of the Crab itself. However, there were many observations, the sky did not change much while data sets 3 and 4 were acquired, and the bright Hg I λ 4358, Hg I λ 5460, and [O I] λ 5577 night-sky features practically disappeared in the subtraction process (see Fig. 3). This indicates that sky subtraction has not caused errors worse than a few percent in the continuum flux estimates.

(6) Instruments of the IDS type can have slightly nonlinear response characteristics, as noted by Rosa (1985),

Wampler (1985), Davidson and Kinman (1985), and Massey and DeVeny (1986). No corrections for nonlinearity have been made in the measurements discussed above. For some applications, one can assume $R \sim I^{1+\delta}$, where I is intensity, R is instrumental response, and δ is typically of the order of 0.03 or 0.04. In the observations reported here, values of I for flux-calibration stars were larger than those for the Crab by factors of several hundred. If $\delta = 0.03$, and taking underlying sky brightness into account, then the continuum flux noted earlier would be an underestimate by a factor of about 0.85. The corrected value would be within 10% of Kirshner's (1974) measurement. However, this would not explain the discrepant [O III]/continuum ratio emphasized above, which is not seriously affected by slight nonlinearity. The numbers quoted in Sec. III above imply that nonlinearity has not caused the [O III] flux to be seriously underestimated here. Either the instrument is nearly linear or else its nonlinearity has been balanced by the other possible errors discussed above.

An attempt was made to calibrate the nonlinearity of the Mount Lemmon IDS. Numerous daytime integrations on an emission-line lamp, alternately with and without a superimposed continuum, were used for this purpose. (If the response is nonlinear, then the average response ratios between bright and faint emission lines should depend upon whether there is a strong underlying continuum.) This test circumvents the effects of lamp fluctuations by using many independent observations, and it does not require an independent photometric device; on the other hand, a very long cumulative integration time is required to attain adequate signal/noise ratios with a strong underlying continuum. The same test had been used in February 1984 to demonstrate nonlinearity in the Kitt Peak IIDS, later confirmed by Massey and DeVeny (1986). Surprisingly, results with the Mount Lemmon instrument were consistent with a linear response, essentially $\delta \approx 0.00 \pm 0.02$, but the precision of this result is unsatisfying. Another test is available. A few galaxies were observed during the January 1985 Mount Lemmon observing run, and two of them, NGC 4861 and Arp 233, had strong enough emission lines to give accurate measurements of the apparent [O III] λ 5007/ λ 4959 ratio with only weak underlying continua. Four such independent measurements gave a ratio 3.04 ± 0.04 . The theoretical intrinsic ratio is not known precisely enough, but the Kitt Peak IIDS consistently gives a response ratio (λ 5007/ λ 4959) ≈ 3.1 (Davidson and Kinman 1985) and probably has a nonlinearity parameter $\delta \approx 0.026$ (Massey and DeVeny 1986). Thus the smaller response ratio for the Mount Lemmon IDS, 3.04 ± 0.04 , seems to hint that $\delta \approx 0.01 \pm 0.01$ for the data reported here, in which case the continuum deficiency discussed above is not explained merely by instrumental nonlinearity. (*Caveat:* The value of δ for continuum measurements may differ from the value that applies to emission lines; the effect is not understood and may be quite complicated, but the tests noted above do seem to indicate qualitatively, at least, that the Mount Lemmon IDS was more nearly linear than the Kitt Peak IIDS.)

Because of the combined uncertainties listed above as well as uncertainties in previous measurements, no changes in the Crab's continuum or [O III] fluxes have been *proven* in a strict sense. However, if one considers only the actual measurements—those by O'Dell, Kirshner, Davidson, Crane, and Chincarini, and those reported here—without being influenced by theoretical expectations, the simplest conclusion

is that the Crab's continuum flux has changed in recent years. Alternatively, a significant visual-wavelength continuum halo may exist just outside the [O III] boundary, or (less likely) the [O III] flux may have changed. Each of these possibilities is unexpected and is of great theoretical importance. If the apparent flux discrepancies are illusory, then all existing data are unsuitable for assessing the true nebular brightness and its rate of change. In summary, the above discussion clearly demonstrates the need for careful, improved measurements!

The smoothness of the continuum spectrum is potentially interesting. Data sets 2 and 3 have good enough wavelength coverage, spatial coverage, and sky subtraction to be useful in this regard. Relative continuum measurements from these data sets are plotted in Fig. 5. The plotted values have been measured by direct comparisons with Feige 15 and Feige 34 at the same wavelengths where Stone (1977) sampled these two calibration stars; this procedure avoids artificial waviness (e.g., polynomial or spline-fitting errors) in the flux calibration. At some wavelengths, notably 5000 Å, interpolations have been used to eliminate emission lines. Continuum measurements by O'Dell (1962) and by Kirshner (1974) are also shown in Fig. 5. All of these are corrected for atmospheric extinction but not for interstellar extinction. The most important result is that irregularities in the previous data, such as Kirshner's depression around 4600 Å, are not confirmed. (Scargle (1969) also found smooth continua at various locations within the Crab. Figure 5 implies that O'Dell's and Kirshner's data are no better than the data reported here for assessing continuum fluxes—besides disagreeing with each other, they are not smooth enough.)

The apparent continuum is perceptibly curved in a log-log plot (bottom of Fig. 5), but this is partly because of the shape of the interstellar extinction curve. The intrinsic continuum is practically indistinguishable from a power law in this limited wavelength range. The continuum found here is slightly "bluer" than the spectra reported by previous authors. Assuming that this is not a real change since the early 1970s, it may indicate a systematic color error in the flux calibration, conceivably involving a wavelength-dependent nonlinearity parameter δ . Similar effects have been noted before (Davidson and Kinman 1985).

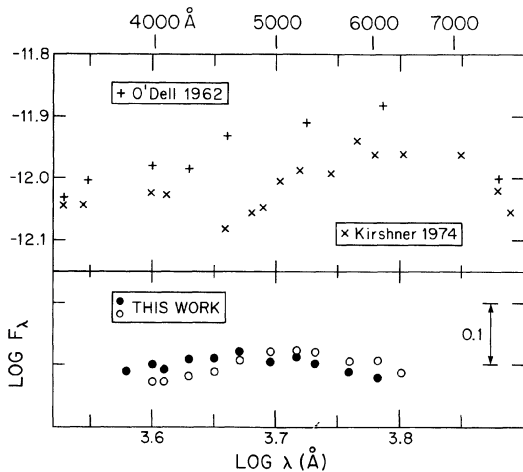


FIG. 5. (Bottom) Relative continuum fluxes: \circ data set 2, \bullet data set 3. (Top) Absolute continuum fluxes from the Crab reported by O'Dell (1962) and by Kirshner (1974). Points in this figure are corrected for atmospheric extinction but not for interstellar extinction.

VI. DISCUSSION

If the continuum flux trend suspected in Sec. V is real, it must have serious implications for models of the nonthermal nebula and pulsar (see Coroniti and Kennel 1985, and other references cited in Kafatos and Henry 1985 and in DF). The main reason for skepticism regarding this trend is the theoretical unexpectedness of such a rapid rate of decline, 1% per year or faster. However, there is no obvious theoretical reason to rule out such an effect at visual wavelengths, where the radiating particles can have lifetimes less than the age of the nebula. The visual and ultraviolet continuum accounts for much of the Crab's luminosity but does not fit smoothly onto either the x-ray or the radio continua (see Sec. 2 of DF). Therefore, even though the data are not quite good enough to prove the effect, we cannot dismiss the apparent trend from O'Dell (1962) to Kirshner (1974) to the data reported here. Of course, there may be alternative interpretations as sketched in Sec. V above. The safest conclusion, already emphasized in DF, is that *precise specialized measurements of the Crab's total visual-wavelength brightness are urgently needed*. Even if such observations contradict the suspicions expressed above, they will be useful in a positive sense, in providing initial data that we will eventually need in order to find the actual secular rate of change.

Ordinary *UBVRI* photometry is unsuitable for the Crab because of the emission lines; interference filters must be used instead. A good continuum interval to sample would be 5200–5400 Å, which contains no bright nebular or night-sky emission lines (although some weak nebular [Fe II] and [Fe III] emission is present there, see Fesen *et al.* 1978). The best approach may be to use a modern imaging detector on a small telescope, with provision for polarization effects. Absolute flux calibrations are desired, but for detecting small changes it would be useful to have extremely precise comparisons with stars close to the Crab even if those stars are not standard flux references. For such comparisons perhaps the stars should be defocused in order to obtain surface brightnesses comparable to that of the Crab; tests for nonlinear detector response are advisable in any case. Altogether, a project of this type is ambitious but should be feasible with equipment now available at many observatories. Similar imaging may be used to seek a faint circumnebular halo.

Another interesting result, unexpected but not really very surprising, is that the He II λ 4686/H β intensity ratio for the whole nebula is larger by a factor of 1.5 to 2 than the value in a typical bright nebular filament (compare Table III with Table 5 of Davidson 1979). The [O III]/H β ratio is also quite large. Probably these ratios indicate the presence of inconspicuous high-ionization gas, possibly accounting for much of the total nebular mass. Such gas may occur as low-density material around the bright filaments.

The emission-line spectrum estimated in Sec. IV is useful for estimating the chemical composition and mass of the Crab Nebula. However, improved photoionization calculations as well as a density survey using [O II] are needed for such analyses (see DF). It should be obvious that the observations reported here can be superseded through the use of a better instrument on a telescope of similar or even smaller size.

Finally, the detection of a "halo" around the Crab continues to elude us. The limits placed in Sec. III above are only mildly restrictive, because even a large amount of gas can have a very small emission measure and surface brightness if its density is low. The high temperature and high ionization

of such gas are unfavorable for detection via emission lines. *Extremely* thorough imaging in search of a halo in the light of the [O III], H α , and even He II lines, and in the continuum as well, is nevertheless worth the effort.

I am especially grateful to R. L. Pennington for his assis-

tance in making the Mount Lemmon telescope and IDS behave properly and for help with the data-reduction routines. Many valuable discussions with R. A. Fesen have also contributed to this work, which was supported by NSF grant AST85-17927.

REFERENCES

- Aller, H. D., and Reynolds, S. P. (1985). In *The Crab Nebula and Related Supernova Remnants*, edited by M. Kafatos and R.B.C. Henry (Cambridge University, Cambridge), p. 75.
- Chevalier, R. A. (1977). In *Supernovae*, edited by D.N. Schramm (Reidel, Dordrecht), p. 53.
- Clark, D. H., Murdin, P., Wood, R., Gilmozzi, R., Danziger, J., and Furn, A. W. (1983). *Mon. Not. R. Astron. Soc.* **204**, 415.
- Coroniti, F. V., and Kennel, C. F. (1985). In *The Crab Nebula and Related Supernova Remnants*, edited by M. Kafatos and R. B. C. Henry (Cambridge University, Cambridge), p. 25.
- Davidson, K. (1979). *Astrophys. J.* **228**, 179.
- Davidson, K., Crane, P., and Chincarini, G. (1974). *Astron. J.* **79**, 791.
- Davidson, K., and Fesen, R. A. (1985). *Annu. Rev. Astron. Astrophys.* **23**, 119.
- Davidson, K., Gull, T. R., Maran, S. P., Stecher, T. P., Fesen, R. A., Parise, R. A., Harvel, C. A., Kafatos, M., and Trimble, V. L. (1982). *Astrophys. J.* **253**, 696.
- Davidson, K., and Kinman, T. D. (1985). *Astrophys. J. Suppl.* **58**, 321.
- Fesen, R. A., Kirshner, R. P., and Chevalier, R. A. (1978). *Publ. Astron. Soc. Pac.* **90**, 32.
- Gull, T. R., and Fesen, R. A. (1982). *Astrophys. J. Lett.* **260**, L75.
- Hayes, D. S., Marko, G. E., Radick, R. R., Rex, K. H., and Greenberg, J. M. (1973). In *Interstellar Dust and Related Topics*, IAU Symposium No. 52, edited by J. M. Greenberg and H. C. van de Hulst (Reidel, Dordrecht), p. 83.
- Kafatos, M., and Henry, R. B. C., editors (1985). *The Crab Nebula and Related Supernova Remnants* (Cambridge University, Cambridge).
- Kirshner, R. P. (1974). *Astrophys. J.* **194**, 323.
- Kristian, J. (1978). *Bull. Am. Astron. Soc.* **10**, 425.
- Massey, P., and DeVeny, J. (1986). *Natl. Opt. Astron. Obs. Newsl. No. 6*, p. 9.
- Matveenko, L. I. (1984). *Sov. Astron. Lett.* **10**, 44.
- Middleditch, J., Pennypacker, C. R., and Burns, M. S. (1987). *Astrophys. J.* **315**, 142.
- Miller, J. S. (1978). *Astrophys. J.* **220**, 490.
- Murdin, P., and Clark, D. H. (1981). *Nature* **294**, 543.
- O'Dell, C. R. (1962). *Astrophys. J.* **136**, 809.
- Oort, J. H., and Walraven, T. (1956). *Bull. Astron. Inst. Neth.* **12**, 285.
- Pequignot, D., and Dennefeld, M. (1983). *Astron. Astrophys.* **120**, 249.
- Rosa, M. (1985). *ESO Messenger No. 39*, p. 15.
- Savage, B. D., and Mathis, J. S. (1979). *Annu. Rev. Astron. Astrophys.* **17**, 73.
- Scargle, J. (1969). *Astrophys. J.* **156**, 401.
- Scargle, J. (1970). *Publ. Astron. Soc. Pac.* **82**, 388.
- Stone, R. P. (1977). *Astrophys. J.* **218**, 767.
- Trimble, V. L. (1977). *Astrophys. Lett.* **18**, 145.
- Velusamy, T. (1984). *Nature* **308**, 251.
- Wampler, E. J. (1985). *ESO Messenger No. 41*, p. 11.
- Wilson, A. S., and Weiler, K. W. (1982). *Nature* **300**, 155.
- Woltjer, L., and Véron-Cetty, M.-P. (1987). *Astron. Astrophys.* **172**, L7.